Localization of the NTUA Emulator Space Robot Using a Discrete Extended Kalman Filter, Data Fusion & Feedback Delay Compensation

Aris Kalgreadis[(1)], Iosif S. Paraskevas[(2)], Thaleia Flessa[(3)] and Evangelos G. Papadopoulos[(4)]

National Technical University of Athens
Department of Mechanical Engineering – Control Systems Laboratory
9 Heroon Polytechneiou Str., 15780, Athens, Greece
e-mail: [(1)]akalgre@gmail.com, [(2)]isparas@mail.ntua.gr, [(3)]tflessa@mail.ntua.gr, [(4)]egpapado@central.ntua.gr

ABSTRACT

On-Orbit Servicing plays a key role in the exploitation of space. To study related issues, the NTUA has developed a Space Robot Emulator for free-flying robotic servicers. In this emulator, the fusion of data from an overhead camera and on-board optical sensors is particularly challenging. This becomes more complex due to the large time delay induced by the camera and image processing. To cope with these challenges, a Discrete Extended Kalman Filter (DEKF) is developed and analyzed. Methods for reducing camera distortion errors and for calibration are discussed and simulation results are presented. Experiments validating the developed methodology are included.

1. INTRODUCTION

On-Orbit Servicing (OOS) and Active Debris Removal (ADR) can benefit by the development of space robotic systems. However, their complex dynamics and control issues must be addressed before their deployment in space. To this end, extensive studies and experiments on simulators and emulators are necessary. A planar Space Emulator has been developed at the NTUA to emulate the operation of free-flying robotic servicers. In the current configuration, it consists of two robotic systems that hover over a flat granite table using air-bearing technology. The robots are being used in studying concepts such as docking strategies, cooperative manipulation, control methodologies in the presence of flexibilities and robot localization [1].

The emulator uses a system of on board optical sensors in parallel to an overhead camera. The optical sensors have a high sampling rate and provide relative localization data but are subject to drift over time. The overhead camera has a lower sampling rate and provides absolute localization data but is subject to image processing delays and image distortion errors. The first challenge is the processing and fusion of data information from these different kinds of sources. To improve localization and attitude estimation, the sensors information should be filtered optimally, reducing measurement noise that degrades position estimation, especially when relative feedback is used. A second challenge towards reducing errors is the large time delay of the overhead camera measurements, caused by image processing, the algorithmic analysis by the off-board computer, and the wireless transmission of the data to the robot. This delay does not permit direct fusion of camera position and attitude estimates to optical sensor estimates.

The first task is to ensure the removal of optical distortions of the camera. Various methods exist using grids with known coordinates in order to define the extrinsic and intrinsic parameters of the camera, for example see [2]. Usually these methods use the pinhole model that may introduce large errors when the distortion is highly non-linear. Other methods calculate these parameters using multiple projections of the same scene [3], or rely on the fact that the lines should have no curvature after the removal of distortions [4]. In this paper an alternative method is being used, based on [5], where a simplified model is satisfactory, thus the parameters can be found by using only one picture of the calibration grid.

Data fusion and filtering of data is usually based on the seminal work of Kalman [6]. Its use in non-linear systems is beyond doubt. Due to its efficiency and practicality, it has been used in several applications [7, 8]. In robotics it is being used also for the exploitation of multiple data sets in order to estimate the localization information. An interesting analysis of alternative methods of Kalman Filter using data fusion can be found in [9], and a comparison in [10]. To cope with the limitations for the NTUA Space Emulator discussed earlier, a Discrete Extended Kalman Filter (DEKF) was developed to fuse camera and optical sensor data using the kinematic model of the robot and centralized measurement fusion techniques. The problem of fusing two different kinds of data, with and without delay, is tackled based on a method which allows direct fusion of the delayed measurement after the calculation of a corrective term during the delay period which is added to the state vector at the end of the delay period. Experiments on the Space Emulator were employed to assess the filter's performance. The obtained accuracy of the sensors is evaluated using a PhaseSpace mocap.

In Section 2 a brief description of the NTUA Space Emulator is presented. Emphasis is given in the localization sensors. The DEKF is analyzed in Section 3. In Section 4, simulations are shown which prove the validity of the developed theory and experiments with the Space Emulator are being presented. Section 5 concludes the work.

2. DESCRIPTION OF THE NTUA EMULATOR

The NTUA Space Emulator consists of two robots that hover over a granite table of minimum roughness. The robots are supported by three porous air-bearings, Fig. 1. The design resembles the basic elements of orbital systems: it includes thrusters, a reaction wheel, localization sensors, processing units, batteries and manipulators. More information can be found in [1]. The following analysis focuses on the elements that are of particular interest for the purposes of this work.

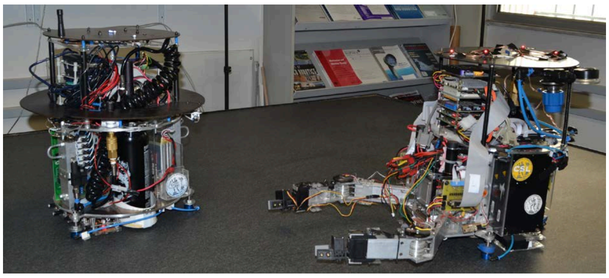

Figure 1. The NTUA Space Robot Emulator. On the right the first robot (used in the experiments of this paper). On the left the new robot.

2.1 Kinematic Model

The robot is equipped with two types of actuators, thrusters and a reaction wheel. The translational and rotational movement is achieved via the forces from the six thrusters, $F_i, (i = 1 \ldots 6)$, and the torque T from the reaction wheel as shown in image, Fig. 2.

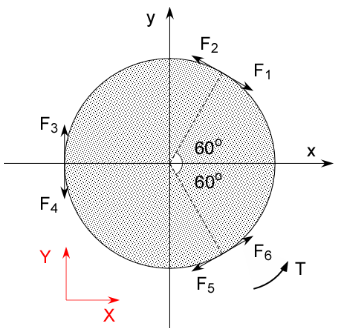

Figure 2. Forces and torques on the robot (without manipulators).

Due to the air bearings the robot can move without friction and therefore simulate movement in space. The equations describing the kinematic model are:

$$\begin{aligned} M \cdot a_x &= F_x \\ M \cdot a_y &= F_y \\ J \cdot \ddot{\theta} &= M_z \end{aligned} \quad (1)$$

where M, J is the mass and inertia of the system, $\alpha_x, \alpha_y, \ddot{\theta}$ the translational and rotational accelerations and F_x, F_y, M_z are the sum of the forces and moments on the robot.

The six thruster forces are always non-negative. In order to simplify the system model, the geometrical symmetry can be used to define these forces as couples that can either take positive or negative values,

$$\begin{aligned} F_a &= F_1 - F_2 \\ F_b &= F_3 - F_4 \\ F_c &= F_5 - F_6 \end{aligned} \quad (2)$$

The effect of these forces and the torque T from the reaction wheel can be analyzed and written in a matrix form as

$$\begin{bmatrix} M \cdot a_x \\ M \cdot a_y \\ J \cdot \ddot{\theta} \end{bmatrix} = \begin{bmatrix} F_x \\ F_y \\ M_z \end{bmatrix} = \mathbf{R}(\theta) \cdot \mathbf{A} \cdot \mathbf{u} \quad (3)$$

where $\mathbf{R}(\theta)$ is the rotation matrix between the world coordinate system, CS{w} and the robot coordinate system CS{r},

$$\mathbf{R}(\theta) = \begin{bmatrix} \cos(\theta) & -\sin(\theta) & 0 \\ \sin(\theta) & \cos(\theta) & 0 \\ 0 & 0 & 1 \end{bmatrix} \quad (4)$$

$\mathbf{u} = \begin{bmatrix} F_a & F_b & F_c & T \end{bmatrix}^T$ is the simplified input vector and $\mathbf{A}$ is the transmission matrix from thruster forces and reaction wheel torque to F_x, F_y, M_z which for the model of this robot has the form

$$\mathbf{A} = \begin{bmatrix} \sin(60^0) & 0 & \sin(60^0) & 0 \\ -\cos(60^0) & 1 & \cos(60^0) & 0 \\ -R & -R & R & 1 \end{bmatrix} \quad (5)$$

where R is the radius of the robot base.

2.2 Optical Sensors

The optical sensors are used for relative measurements. They are the same sensors that are being used as optical mice in computers. Their operational principle relies on optical flow techniques, which are beyond the scope of this work. Optical sensors measure the differential displacements δx and δy at each sampling instant, with respect to the body frame of the optical sensor; this is being done by comparing successive surface pictures.

Two sensors can produce four values per instant, and the three unknown parameters (x, y, θ) can be calculated. Generally the sensors have high sampling rate, compact size, good accuracy and low cost. However, their odometric error is accumulated over time. In order to increase the accuracy of the final measurements, three TRUST Retractable Laser Mini Mouse with 1600cpi nominal resolution sensors are mounted beneath the base of the robot at a distance of 2mm from the table in custom-made supports, Fig. 3. Note that a similar construction exists also on the new robot design, however the experiments in this paper have been performed with the first robot. More about the optical sensors can be found in [11].

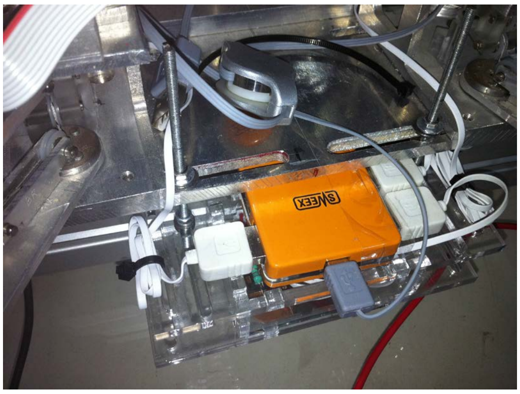

Figure 3. View of an optical sensor installed on a custom-made support.

2.3 Camera

The overhead camera, Fig. 4a, is used for absolute measurements. The position and orientation of the robot is calculated by tracking five LEDs that are placed on the top surface of the robot, Fig. 4b (two of them consist one larger LED). A program was developed which acquires an image from the camera, it processes it via an algorithm where it identifies the LED pattern, remove lens distortion, find the LED coordinates and finally calculate the position and orientation of the robot. In this section the basic principles of the algorithm operation will be described.

Firstly, the algorithm applies a threshold to the image and the pixels that correspond to the LEDs are isolated based on the fact that these pixels have the highest intensity. The coordinates of the pixels (x_{do}, y_{do}) are on the distorted image plane with origin at the corner of the image.

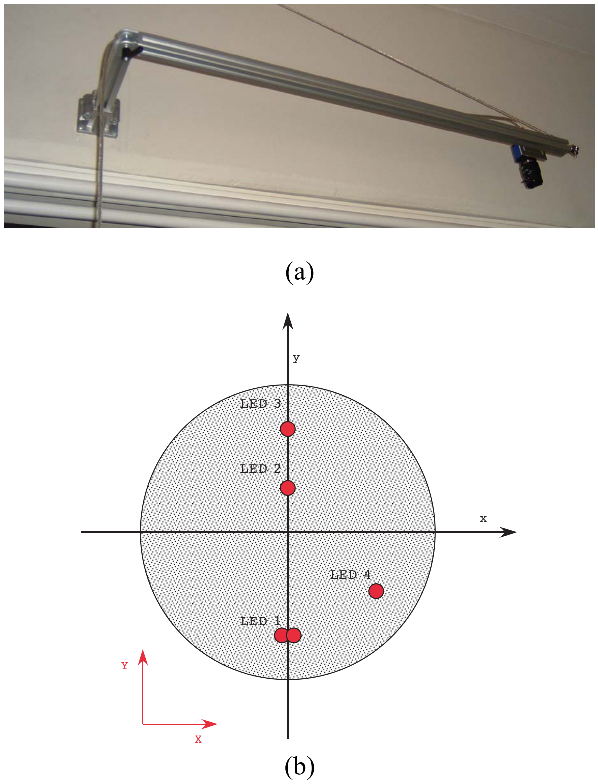

Figure 4. (a) The overhead camera and (b) the LED pattern on top of the robot.

The first step towards removing the lens distortion is to offset the coordinate system in order to make the center of distortion (o_{xi}, o_{yi}) the new origin

$$(x'_{di}, y_{di}) = (x_{do} - o_{xi}, y_{do} - o_{yi}) \tag{6}$$

The aspect ratio of the image is removed by scaling the x-axis by the scale ratio η

$$x_{di} = \eta \cdot x'_{di} \tag{7}$$

The lens distortion is removed and the undistorted pixel coordinates (x_{ui}, y_{ui}) are calculated using

$$\begin{aligned} x_{ui} &= x_{di} \cdot (1 + \kappa \cdot r_{di}^2) \\ y_{ui} &= y_{di} \cdot (1 + \kappa \cdot r_{di}^2) \\ r_{di} &= \sqrt{x_{di}^2 + y_{di}^2} \end{aligned} \tag{8}$$

where κ is the distortion coefficient. Since the robot movement is on a plane and the z coordinate is constant the transformation from undistorted pixels coordinates to *mm* that refer to the CS{w} can be calculated with a simple scale and an offset

$$x_w = \begin{bmatrix} x_{ui} & y_{ui} & 1 \end{bmatrix} \cdot \begin{bmatrix} a_x \\ b_x \\ c_x \end{bmatrix}$$
$$y_w = \begin{bmatrix} x_{ui} & y_{ui} & 1 \end{bmatrix} \cdot \begin{bmatrix} a_y \\ b_y \\ c_y \end{bmatrix} \tag{9}$$

The parameters $o_{xi}, o_{yi}, \eta, \kappa$, used to remove the distortion from the image, were calculated with a calibration method based on [5] that required a single image of a calibration grid. The parameters $a_x, b_x, c_x, a_y, b_y, c_y$, used for the transformation of coordinates where calculated using a linear regression algorithm, with dataset the nodes of the calibration grid. Finally with respect to the known real geometry the pattern of the LEDs can be identified and the position and orientation of the robot can be determined.

Overall even though the camera sensor has low sampling rate and high image processing time, it has good accuracy and can be used along with the optical sensors to improve greatly the localization abilities of the robot.

3. DISCRETE EXTENDED KALMAN FILTER

In order to fuse the measurements from the optical sensors and the camera and use the non-linear kinematic model of the robot a Discrete time Extended Kalman Filter (DEKF) will be developed. In the following analysis, subscript (*o*) refers to optical sensors and (*c*) to the camera.

The state vector for the system is defined as

$$\mathbf{x}_k = \begin{bmatrix} x_k & y_k & \theta_k & \dot{x}_k & \dot{y}_k & \omega_k \end{bmatrix}^{\mathrm{T}} \tag{10}$$

and the control input vector as

$$\mathbf{u}_k = \begin{bmatrix} F_{a,k} & F_{b,k} & F_{c,k} & T_k \end{bmatrix}^{\mathrm{T}} \tag{11}$$

The non-linear kinematic model that describes the change over time of the robots state can be written in the form of a difference equation

$$\mathbf{x}_k = f_{k-1}(\mathbf{x}_{k-1}, \mathbf{u}_{k-1}) + w_k \tag{12}$$

where $f_k(\cdot)$ is the discrete time nonlinear kinematic model of the robot obtained by adding the three velocity states and discretizing the model described in Eq. (3) and $w_k \sim N(0, Q_k)$ is the process noise that is assumed to be white, zero-mean Gaussian with variance Q_k . The measurement model for both sensor systems is linear and is described by the equation

$$\mathbf{z}_k^{(i)} = H \cdot \mathbf{x}_k + v_k^{(i)} \tag{13}$$

where $\mathbf{z}_k = \begin{bmatrix} x_k & y_k & \theta_k \end{bmatrix}^{\mathrm{T}}$ is the measurement vector, $v_k^{(i)} \sim N(0, R_k^{(i)})$ is the process noise of the $i-th$ sensor that is also assumed to be white, zero-mean Gaussian with variance $R_k^{(i)}$ and H is the linear measurement matrix that is the same for both sensor systems

$$H = \begin{bmatrix} 1 & 0 & 0 & 0 & 0 & 0 \\ 0 & 1 & 0 & 0 & 0 & 0 \\ 0 & 0 & 1 & 0 & 0 & 0 \end{bmatrix} \tag{14}$$

The prediction of the new state $\hat{\mathbf{x}}_k(-)$ is calculated using the system model at time step k ,

$$\hat{\mathbf{x}}_k(-) = f_{k-1}(\hat{\mathbf{x}}_{k-1}(+), \mathbf{u}_{k-1}) \tag{15}$$

and the covariance $P_k(-)$ associated with this prediction

$$P_k(-) = A_{k-1} P_{k-1}(+) A_{k-1}^T + Q_{k-1} \tag{16}$$

where

$$A_{k-1} = \left. \frac{\partial f(x,u)}{\partial x} \right|_{x=\hat{x}_{k-1}(+)} \tag{17}$$

is the Jacobian obtained by linearizing about the previous state estimate $\hat{x}_{k-1}(+)$.

Before formulating the measurement update equations we have to define how the filter will handle the measurements from the different sensor systems. The sampling frequency for the camera is $\approx 4Hz$ and for the optical sensors is $125Hz$. To be exact the sampling frequency is 7 Hz, however due to the processing delay, the received data arrive at a frequency of about 4Hz. Note that the optical sensors can have higher frequency. However, this value was chosen as a compromise between the sensing requirements and the execution time required by the robot to execute many different operations (except the data acquisition from the optical sensors). By setting the frequency of the filter to be the same with the optical sensor sampling frequency, two states of operation can be distinguished, either at time step k only a measurement from the optical sensors is available or at another time step k' measurements from both sensors systems are available.

When the only measurements available are from the optical sensors, the measurement update equations are the ones derived in the classic form of the EKF. The Kalman gain K_k in calculated as,

$$K_k = P_k(-)\cdot H^T \cdot \left(H \cdot P_k(-)\cdot H^T + R_k^{(o)}\right)^{-1} \tag{18}$$

so the updated state prediction $\hat{x}_k(+)$ is

$$\hat{x}_k(+) = \hat{x}_k(-) + K_k \cdot \left(z_k^{(o)} - H\cdot \hat{x}_k(-)\right) \tag{19}$$

and finally the associated covariance $P_k(+)$ is

$$P_k(+) = \left(I - K_k \cdot H\right)\cdot P_k(-) \tag{20}$$

When measurements from both the optical sensors and the camera are available, they need to be fused in order to be used in the filter. In this paper a centralized fusion technique is used, Fig. 5, that calculates a single fused measurement model by weighted observation as

$$R_{k'} = \left[R_{k'}^{(c)-1} + R_{k'}^{(o)-1}\right]^{-1} \tag{21}$$

$$H_{k'} = R_{k'} \cdot \left[R_{k'}^{(c)-1}\cdot H + R_{k'}^{(o)-1}\cdot H\right] \tag{22}$$

$$z_{k'} = R_{k'} \cdot \left[R_{k'}^{(c)-1}\cdot z_{k'}^{(c)} + R_{k'}^{(o)-1}\cdot z_{k'}^{(o)}\right] \tag{23}$$

The calculated fused $R_{k'}$, $H_{k'}$, $z_{k'}$ are used in Eq. (18), (19) and (20) to calculate the Kalman gain, the updated state prediction and the associated covariance correspondingly. Furthermore the filter needs to be modified in order to account for the delayed measurements from the camera.

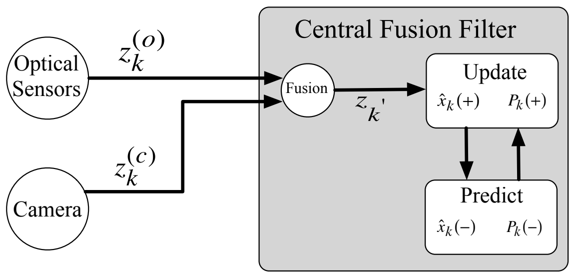

Figure 5. Scheme of the fusion technique used with the proposed DEFK.

This delay is caused by the image processing algorithm and the wireless communication time between the cameras external computer and the robot. The time delay of the camera is calculated around 0.3 s that corresponds to approximately 38 time steps. The method to be used is able to handle large delay times with a computationally efficient and fast way by calculating a corrective term that is added to the filter estimate when the delayed measurement arrives [12].

The first assumption made is that there is a camera measurement taken at time step s but due to the time delay is available at a later time step k and is referred as $z_k^{(c)*}$, Fig. 6. Moreover we make the assumptions that the delay period $N = k - s$ is known and constant and that the measurement variance of the delayed camera measurement $R_s^{(c)*}$ is known at time step s.

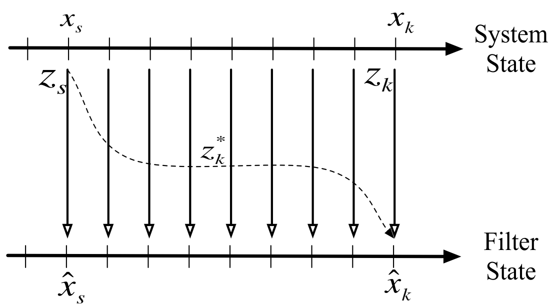

Figure 6. The way the delayed information is treated.

In order to tackle the problem of fusing the delayed measurement, two parallel filters are created. The main filter is a simple EKF filter that uses only measurement from the optical sensors. The parallel filter works only in the period N of the time delay. At time step s, the fused filter covariance matrix is updated using Eqs. (21) and (22), even though the measurement is not yet available. At time k, when $z_k^{(c)*}$ becomes available it is fused using the Eq. (23) and then the following quantity is added to the state estimate

$$\delta\hat{x}_k = M_* \cdot K_s \cdot \left(z_k^{(c)*} - H\cdot \hat{x}_s\right) \tag{24}$$

where M_* is calculated by

$$M_* = \prod_{i=0}^{N-1}(I - K'_{k-i}\cdot H_{k-i})\cdot \Phi_{k-i-1} \tag{25}$$

The K' signifies that these Kalman gains have been calculated in the parallel filter using the covariance matrix of the fused model at time s. The M_* matrix can be calculated incrementally at each time step making it more computationally efficient. At the end of the delay period M_* resets to the identity matrix.

Up until time k estimates from the main filter will be used; at time k when the delayed measurement arrives, the parallel filter will have the correct estimate.

4. SIMULATIONS AND EXPERIMENTS

4.1 Simulations

To test the validity of the proposed DEKF a model in Simulink/Matlab was created. A desired trajectory was designed and the sensor measurements were generated by adding white, zero-mean Gaussian noise to this trajectory. The sampling time of the filter was set equal to the sampling time of the optical sensors $T_s = 0.008s$ and the sampling time of the camera $T_{cam} = 0.304s$. As mentioned in Section 3 the time delay of the camera measurements was approximately 0.3sec so it was set equal to the camera's sampling time. The measurement additive noise variance was set according to experimental observations

$$\begin{aligned} \sigma_{v_k^{(c)}} &= [0.001m\ 0.001m\ 0.0175rad]^T \\ \sigma_{v_k^{(o)}} &= [0.005m\ 0.005m\ 0.0349rad]^T \end{aligned} \tag{26}$$

And the associated variance matrix to be used in the filter $R_k^{(c)} = diag(\sigma_{v_k^{(c)}}{}^2)$ and $R_k^{(o)} = diag(\sigma_{v_k^{(o)}}{}^2)$. The process variance is set to:

$$Q = diag\left(\begin{bmatrix} 1 & 1 & 1.75 & 1 & 1 & 1.75 \end{bmatrix}\right) \cdot 10^{-6} \tag{27}$$

Finally the initial conditions for the simulation were set

$$\begin{aligned} \mathbf{x}_0 &= \begin{bmatrix} 0 & 0 & 0.7854 & 0 & 0 & 0 \end{bmatrix}^T \\ P_0 &= 0.5 \cdot I \end{aligned} \tag{28}$$

The simulation results are presented in Figs. 7 and 8.

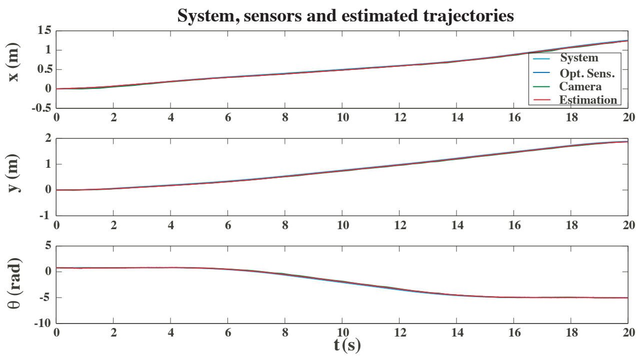

Figure 7. System, sensors and estimated trajectories.

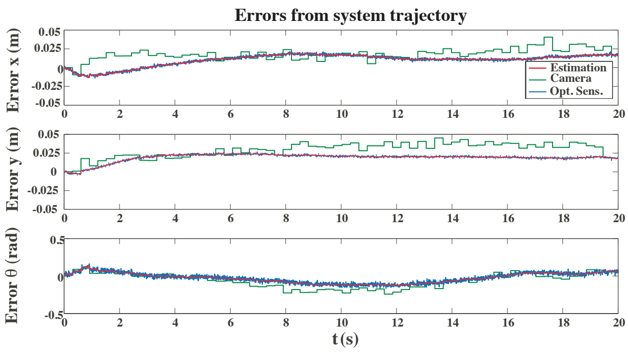

Figure 8. Sensors and estimated errors with respect to system trajectory.

4.2 Experimental results

The filter was also tested using the Simulink model with real data from the sensor systems. Firstly, an open-loop trajectory of a straight line was designed. Then the robot was placed on the granite table with zero initial velocity and executed the open loop movement with thrusting while the camera and the optical sensors where tracking the location of the robot. The measurements were saved and then imported to Simulink for processing. During this experiment the locations of the robot was also tracked by the PhaseSpace mocap for evaluation of the estimated location accuracy.

For this experiment the sampling time of the filter and the optical sensors was set to $T_s = 0.04s$ and the sampling and delay time of the camera $T_{cam} = 0.2640s$. Note that these times are slightly different that the ones used in the simulation but this does not affect the results. The variance matrices for the process and the measurement noises are defined as in the ones describes in the previous section. The initial conditions were set

$$\begin{aligned} \mathbf{x}_0 &= \begin{bmatrix} 0.8731 & 0.5821 & 1.7704 & 0 & 0 & 0 \end{bmatrix}^T \\ P_0 &= 0.5 \cdot I \end{aligned} \tag{29}$$

The experimental results are presented in Figs. 9 and 10.

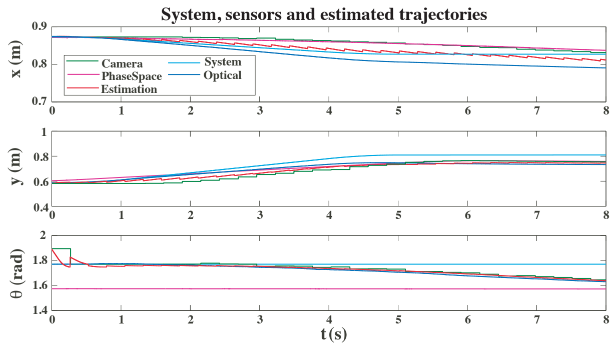

Figure 9. System, sensors and estimated trajectories with real data and Phase Space measurements.

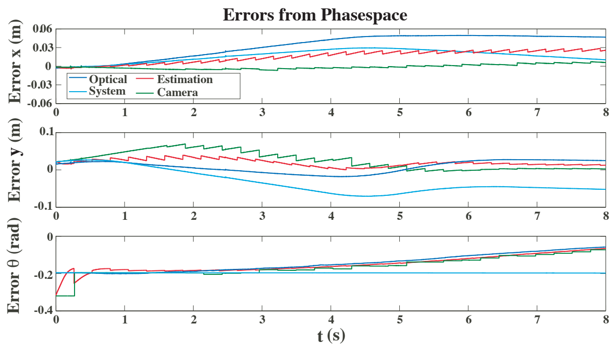

Figure 10. System, sensors and estimated errors with respect to the Phase Space trajectory.

4.3 Discussion

The proposed DEKF can successfully use the kinematic model of the system and fuse the information from the two different sensors to reduce the localization error. The filter utilizes the fast and accurate measurements from the optical sensors and the accumulated drift over time is removed because the error resets every time there is an absolute measurement from the camera. Moreover after the removal of the camera distortion and the modification of the filter to compensate for the delayed measurements the camera measurements are reliable and precise.

In the future, the errors can be reduced by using better calibration techniques for the sensors. These techniques will allow for example to lower the computation cost of the image processing algorithm and subsequently the delay time and calculate a more precise model for the process and measurement noise or will lower the camera distortion effects to a minimum.

5. SUMMARY

In this paper the problem of fusing data from two different kinds of sensors (for relative and absolute measurements), while on the same time one sensor presents delay was addressed. The hardware subsystems of the NTUA Space Emulator were presented with emphasis on the localization subsystem. The procedure to reduce camera distortion was analyzed. The theoretical development of a DEKF with data fusion and time delay was shown. Simulations and experimental results have shown its validity.

ACKNOWLEDGEMENTS

Mr. Paraskevas' research has been co-financed by the European Union (European Social Fund – ESF) and Greek national funds through the Operational Program "Education and Lifelong Learning" of the National Strategic Reference Framework (NSRF) - Research Funding Program: Heracleitus II. Investing in knowledge society through the European Social Fund.

REFERENCES

1. Machairas, K. et al, "Extending the NTUA Space Robot Emulator for Validating Complex On-Orbit Servicing Tasks", *12th Symposium on Advanced Space Technologies in Robotics and Automation (ASTRA)*, ESA/ESTEC, Noordwijk, The Netherlands, 2013.

2. Zhang, Z. Y., "A Flexible New Technique for Camera Calibration", IEEE Transactions on *Pattern Analysis and Machine Intelligence,* 22(11), pp. 1330-1334, 2000.

3. Oliver, F., Luong, Q. T. And Maybank, S., "Camera Self-calibration: Theory and Experiments", *Computer Vision – ECCV'92*, Springer Berlin/ Heidelberf, p.p. 321-334, 1992.

4. Davernay, F. And Faugeras, O., "Straight Lines Have to Be Straight", *Machine Vision and Applications*, No. 13.1, pp. 14-24, 2001.

5. Bailey, D. G., "A New Approach to Lens Distortion Correction", *Proceedings Image and Vision Computing New Zealand*, pp. 59-64, 2002.

6. Kalman, R. E., "A New Approach to Linear Filtering and Prediction", *Journal of Basic Engineering,* No. 82.1, pp. 35-45, 1960.

7. Brown, R. G. and Hwang, P. Y. C., "*Introduction to Random Signals and Applied Kalman Filtering*", 2nd Edition, John Wiley & Sons, Inc., 1992.

8. Grewal, M. S. and Andrews, A. P., "*Kalman Filtering Theory and Practice Using MATLAB*", John Wiley & Sons, 2008.

9. Durrant-Whyte, H., "*Multi Sensor Data Fusion*", Sprigner Handbook of Robotics, 2001.

10. Qiang, G. and Harris, C. J., "Comparison of Two Measurement Fusion Methods for Kalman-Filter-Based Multisensor Data Fusion", *IEEE Transactions on Aerospace and Electronic Systems*, pp 273-279, 2001

11. Flessa T., et al, "Localization and Fuel Management Techniques for the NTUA Space Emulator System", *International Symposium on Artificial Intelligence, Robotics and Automation in Space (i-SAIRAS)*, Turin, Italy, 2012.

12. Larsen, T. D., Andersen, N. A., Ravn, O., & Poulsen, N. K., "Incorporation of time delayed measurements in a discrete-time Kalman filter," in *Decision and Control, 1998. Proceedings of the 37th IEEE Conference*, vol. 4, 1998, pp. 3972-3977.